This article is published as part of the *Dalton Transactions* themed issue entitled:

Computational Chemistry of Molecular Inorganic Systems

Guest Editor: Professor Stuart MacGregor
Heriot-Watt University, Edinburgh, U.K.

Published in issue 42, 2011 of *Dalton Transactions*

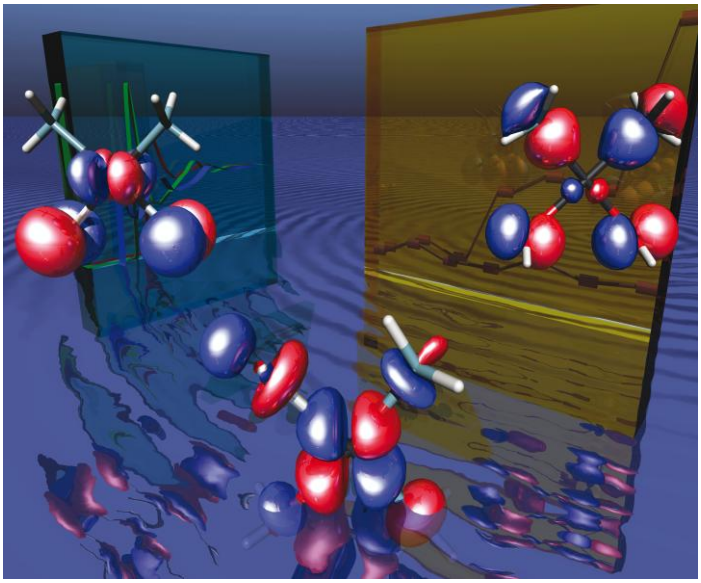

Image reproduced with the permission of Hirofumi Sato

Articles in the issue include:

COMMUNICATION:
Comparison of different ruthenium–alkylidene bonds in the activation step with N-heterocyclic carbene Ru-catalysts for olefins metathesis
Albert Poater, Francesco Ragone, Andrea Correa and Luigi Cavallo
Dalton Trans., 2011, DOI: 10.1039/C1DT10959F

HOT ARTICLES:
Matrix infrared spectroscopic and density functional theoretical investigations on thorium and uranium atom reactions with dimethyl ether
Yu Gong and Lester Andrews
Dalton Trans., 2011, DOI: 10.1039/C1DT10725A

Reductive coupling of carbon monoxide by U(III) complexes—a computational study
Georgina Aitken, Nilay Hazari, Alistair S. P. Frey, F. Geoffrey N. Cloke, O. Summerscales and Jennifer C. Green
Dalton Trans., 2011, DOI: 10.1039/C1DT10692A

Prediction of high-valent iron K-edge absorption spectra by time-dependent Density Functional Theory
P. Chandrasekaran, S. Chantal E. Stieber, Terrence J. Collins, Lawrence Que, Jr., Frank Neese and Serena DeBeer
Dalton Trans., 2011, DOI: 10.1039/C1DT11331C

Visit the *Dalton Transactions* website for more cutting-edge inorganic and organometallic research
www.rsc.org/dalton

Dalton Transactions

Dynamic Article Links

Cite this: *Dalton Trans.*, 2011, **40**, 11080

www.rsc.org/dalton

PAPER

Reductive coupling of carbon monoxide by U(III) complexes—a computational study†

Georgina Aitken,[a] Nilay Hazari,[a] Alistair S. P. Frey,[b] F. Geoffrey N. Cloke,[b] O. Summerscales[b] and Jennifer C. Green*[a]

Received 18th April 2011, Accepted 30th June 2011
DOI: 10.1039/c1dt10692a

The role of U((η-C_8H_6{Si^iPr_3-1,4}$_2$)(η-C_5Me_5) and U((η-C_8H_6{Si^iPr_3-1,4}$_2$)(η-C_5Me_4H) in the reductive di- tri- and tetramerization of CO has been modelled using density functional methods and U(C_8H_8)(C_5H_5) as the metal fragment. The orbital structure of U(C_8H_8)(C_5H_5) is described. CO binding to form a monocarbonyl U(C_8H_8)(C_5H_5)(CO) is found, by a variety of methods, to place spin density on the CO ligand *via* back-bonding from the U5f orbitals. A possible pathway for formation of the yne diolate complex [U(C_8H_8)(C_5H_5)]$_2C_2O_2$ is proposed which involves dimerization of U(C_8H_8)(C_5H_5)CO *via* coordination of the CO O atoms to the opposing U atoms followed by C–C bond formation to form a zig-zag intermediate, stable at low temperatures. The intermediate then unfolds to form the yne diolate. The structures of [U(C_8H_8)(C_5H_5)]C_2O_2, the deltate complex [U(C_8H_8)(C_5H_5)]C_3O_3 and the squarate complex [U(C_8H_8)(C_5H_5)]C_4O_4 are optimized and provide good models for the experimental compounds. The reaction of further CO with a zig-zag intermediate to form deltate and squarate complexes was explored using Th(C_8H_8)(C_5H_5) as a model and low energy pathways are proposed.

Introduction

The long-established Fischer–Tropsch process[1] is employed on a very large scale to effect the conversion of synthesis gas (CO/H_2) to hydrocarbons and oxygenates, and continues to attract considerable interest.[2] The C–C coupling reactions implicit in the latter have been extensively modelled using molecular organometallic systems,[3] for example the formation of enediolate complexes[4–6] or ethene[7] from reactions of early transition metal or f-block hydrides with CO. Evans has also described the reductive trimerisation of CO by organo-samarium and lanthanum complexes to afford ketene carboxylate derivatives.[8,9] In 2006 we reported a novel CO coupling reaction not previously observed in Fischer–Tropsch chemistry, namely the reductive cyclotrimerisation of CO by the U(III) complex [U(η-C_8H_6{Si^iPr_3-1,4}$_2$)(η-Cp*)(THF)] to afford the deltate, oxocarbon complex [U(η-C_8H_6{Si^iPr_3-1,4}$_2$)(η-Cp*)]$_2$(μ-η^1:η^2-C_3O_3) (Scheme 1).[10]

We also found that slight modification of the ligand environment around uranium (replacement of C_5Me_5 with C_5Me_4H) resulted in the reductive cyclotetramerisation of CO to afford the squarate derivative [U(η-C_8H_6{Si^iPr_3-1,4}$_2$)(η-C_5Me_4H)]$_2$(μ-η^2:η^2-C_4O_4) with 100% selectivity (Scheme 2).[11]

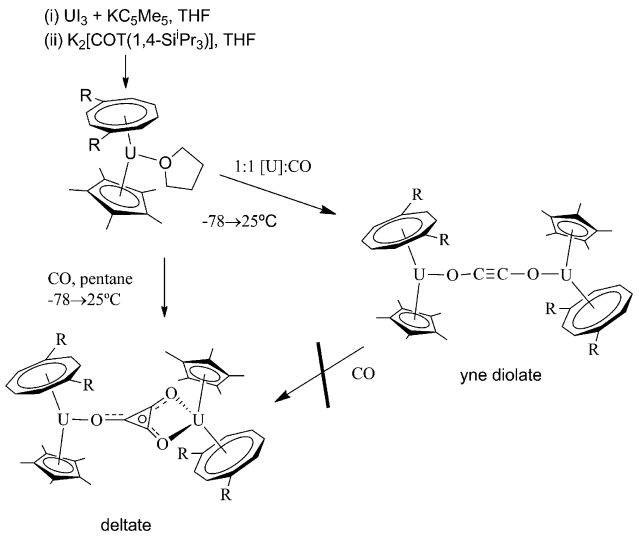

Scheme 1

Subsequent experimental and preliminary computational studies suggested that these reductive cyclooligomerisation reactions of CO proceed *via* a reactive, dimeric C_2O_2 intermediate which then adds further CO to form the uranium deltate or squarate derivatives. In the absence of further CO, the reactive intermediate transforms into a linear yne diolate complex [U(η-C_8H_6{Si^iPr_3-1,4}$_2$)(η-Cp*)]$_2$(μ-η^1:η^1-C_2O_2), which is stable (Scheme 1).[12] However, the yne diolate does not react with further CO so is not an intermediate in deltate formation.

[a]*Department of Chemistry, Oxford University, Inorganic Chemistry Laboratory, South Parks Road, Oxford, UK, OX1 3QR. E-mail: jennifer.green@chem.ox.ac.uk*
[b]*The Chemistry Division, School of Life Sciences, University of Sussex, Brighton, UK, BN1 9QJ*

† Electronic supplementary information (ESI) available. See DOI: 10.1039/c1dt10692a

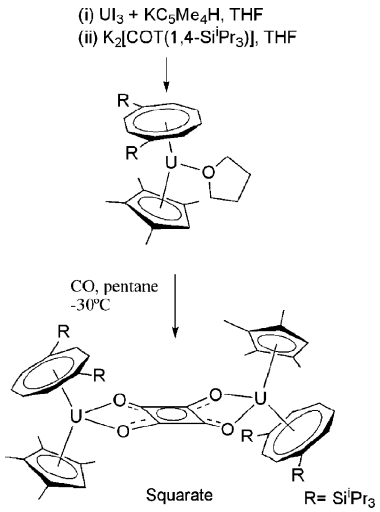

Scheme 2

Calculations on actinide complexes are undoubtedly among the most challenging because they are frequently open shell, and both relativistic and correlation effects are important. High level *ab initio* treatments have been applied successfully to small molecules but for the class of larger systems considered here density functional methods have proved a useful guide to structure and mechanism. The reader is directed to a number of excellent recent reviews of actinide computational methods and results.[13–16]

In this paper we present computational evidence for various intermediates in the formation of the yne diolate, deltate and squarate complexes and estimates of the energy profile of the reactions. Part of this work has been the subject of preliminary communications.[10–12]

Results and discussion

All calculations have been carried out on a model system with the fragment M(η-C_8H_8)(η-C_5H_5) (abbreviated MCotCp; M = U or Th).

UCotCp

The starting material for reductive CO coupling may be either the THF adduct as illustrated in Schemes 1 and 2 or the unsolvated U((η-C_8H_6{Si^{i}Pr$_3$-1,4}$_2$)(η-C_5R_5) (R_5 = Me_5, Me_4H), presumably THF decoordinates prior to reaction with CO.

Geometry optimization of UCotCp, with $S = 3/2$, gave a bent structure, **1**, with non-parallel rings.

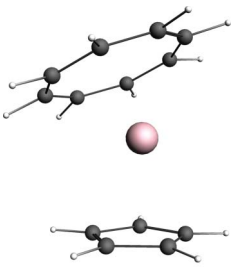

1

The U–C distances to the Cot ring ranged from 2.639 Å to 2.693 Å (average 2.644 Å) and those to the Cp ring from 2.678 to 2.745 Å (average 2.710 Å). A solvent free analogue has not been crystallographically characterized but the 4,4′-dimethyl-2,2′-bipyridine derivative of U(η-C_8H_8)(η-C_5Me_5) shows average distances of 2.703 (U–C_{Cot}) and 2.752 (U–C_{Cp^*})[17] and the THF derivative of U(η-C_8H_6{Si^{i}Pr$_3$-1,4}$_2$)(η-C_5Me_5) has U–C distances of 2.708 (U–C_{Cot}) and 2.774 (U–C_{Cp^*}).[10] The discrepancies in U–C distance between our calculation and the X-ray diffraction results may in part be due to the lack of substituents in our model but are mainly occasioned by the absence of other coordinating groups, *vide infra.*

Isosurfaces for the occupied α spin orbitals are shown in Fig. 1. The three unpaired electrons occupy essentially 5f orbitals; a small amount of back-donation to the Cp ring is evident in two of these but the C 2p character is <4%. At lower energies α and β spin orbitals are very similar and both are occupied. The pairs of orbitals binding the Cot ring are of δ symmetry; notably the U contribution to these bonding orbitals is of 12% 6d character and 5% 5f character. Below these lie π symmetry orbitals binding the Cp ring which have 9% U 6d character.

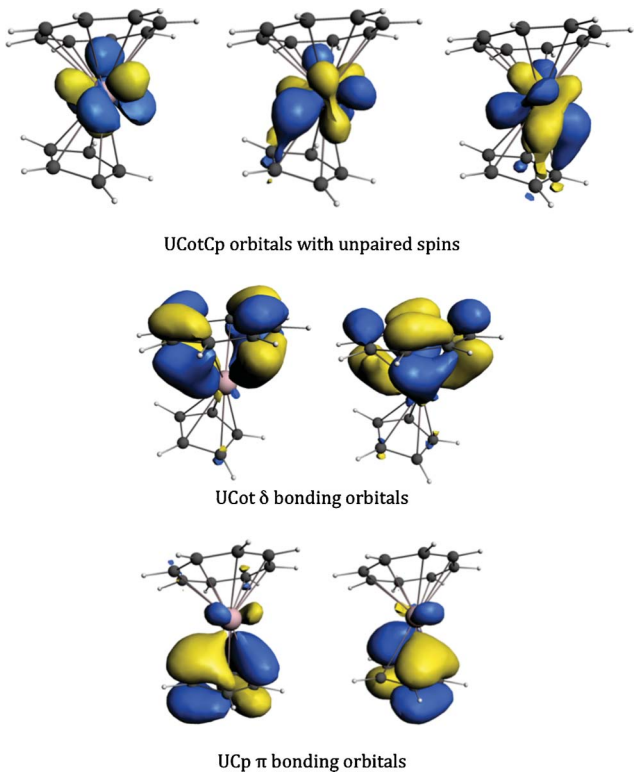

Fig. 1 Isosurfaces of the α spin orbitals of UCotCp.

UCotCpCO

The reductive coupling reactions to the yne diolate and deltate dimers can be initiated by either the solvent free U(η-C_8H_6{Si^{i}Pr$_3$-1,4}$_2$)(η-C_5Me_5) or the THF adduct, U((η-C_8H_6{Si^{i}Pr$_3$-1,4}$_2$)(η-C_5Me_5)THF. The first step in any of the reaction sequences is presumed to be binding of CO to UCotCp to form UCotCpCO. Experimental evidence for this, is observation of an IR band at 1920 cm^{-1} when CO is added to U((η-C_8H_6{Si^{i}Pr$_3$-1,4}$_2$)(η-C_5Me_5)

at −78 °C.[12] The signal decays within 15 min at room temperature so the monocarbonyl has not been isolated.

Three modes of coordination of CO to UCotCp were investigated, C bound (**2**), O bound (**3**) and η^2-side-on bound (**4**), and minima were found for all three. The C bound CO was found to be the lowest in energy. The model **2** showed average U–C distances for the cot ring of 2.698 Å and for the cp ring of 2.737 Å, closer to those found for the bipyridine and THF adducts described above. Thus on coordination of an extra ligand it appears that the U-ring distances lengthen. Structures, energetics and CO wavenumbers are shown in Fig. 2.

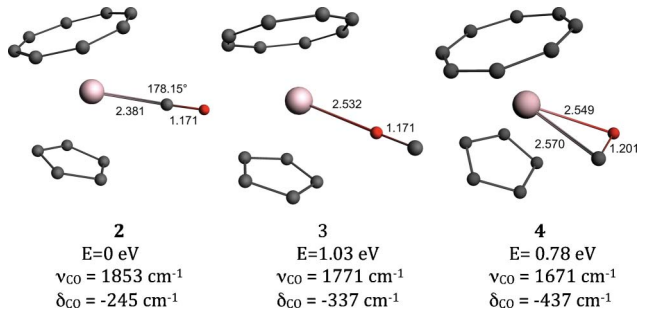

Fig. 2 Structures calculated for various isomers of UCotCpCO and the calculated relative energies (E) and CO stretching wavenumbers (ν_{CO}) together with differences from that calculated for CO (δ_{CO}).

Reported distances for U(η-$C_5H_nMe_{5-n}$)$_3$CO are 2.383(6) Å (U–CO) and 1.142(7) (C–O) when $n = 1$[18] and 2.485(9) Å (U–CO) and 1.13(1) (C–O) when $n = 0$.[19] Thus the calculated U–CO distance for **2** is similar to that found for U(η-C_5HMe_4)$_3$CO. The CO stretch for U(η-C_5HMe_4)$_3$CO is media dependent being 1880 cm^{-1} in the solid state and 1900 cm^{-1} in petroleum ether solution, thus showing shifts of −263 cm^{-1} and −243 cm^{-1} from free CO.[18] The shift observed from free CO in the case of U((η-C_8H_4{Si^{i}Pr$_3$-1,4}$_2$)(η-C_5Me_5)CO is −223 cm^{-1}. The similarity of the data together with the energy predictions from the calculations suggest that the CO is also C bound in the latter case.

An MO diagram, which indicates the level shifts on CO binding, is given in Fig. 3. Both the 5f orbitals and the upper ligand levels are stabilized on CO binding, the former rather more so. Of the three unpaired electrons, two are delocalized into the CO 2π orbitals accounting for the reduction in CO stretching frequency from free CO (Fig. 2). Mulliken population analysis indicates orbital 28a′ has 7% C 2p and 5% O 2p character and orbital 17a″ 18% C 2p and 11% O 2p character. Mulliken analysis gives the unpaired spin density as 0.27 on C and 0.14 on O.

The CO binding found for **2** is in contrast with that calculated for the tris-cyclopentadienyl uranium carbonyl series, UCp$^R{}_3$CO (Cp^R = C_5H_5, $C_5H_4SiMe_3$, C_5HMe_4, C_5Me_5).[20] In these cases the unpaired spins were localized in metal f orbitals and the back-bonding originated from filled cyclopentadienyl based orbitals of π symmetry. Evidence cited for this model was the large sensitivity of the CO stretch to the ligand substituent, which was well reproduced by the calculations. These calculations employed the B3PW91 functional and the Stuttgart–Dresden–Bonn small-core basis sets for U, 6-311G* basis sets for the C and O of CO, 6-31G(d,p) basis sets for the ring C and H atoms and Si with a large core and 4s3pid basis set.[20] Given the possibility that the results found for UCotCpCO are model dependent, further calculations

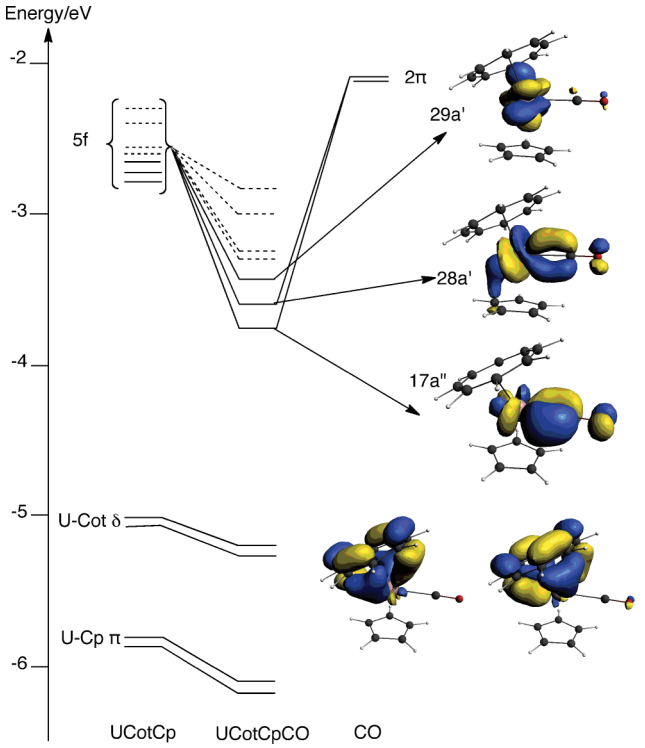

Fig. 3 Calculated MO energy level diagram and orbitals of UCotCp. Levels are shown for alpha spin orbitals, dashed levels indicate virtual orbitals.

were carried out using a using a number of different functionals and basis sets (Table 1). These included the hybrid functional B3LYP and all electron TZP basis sets, the BP86 functional and SDD basis sets and finally the B3PW91 functional with SDD basis sets (the latter two calculations employed the Gaussian[21] program suite). The results are compared in Table 1.

Change of basis set and relativistic approximation had little effect on the U–CO and C–O distances. Use of the hybrid functional B3LYP resulted in a longer U–CO and shorter C–O distance whereas the B3PW91 functional gave shorter U–CO and C–O distances. However in all cases significant spin density was found on the carbonyl ligand.

The localization of the three unpaired electrons on the U in the UCp$^R{}_3$CO series is attributed to the trigonal symmetry of the molecule. Three 5f orbitals, two of δ symmetry and one of ϕ symmetry are non-bonding with respect to the Cp^R rings and are occupied by the three unpaired spins. These are not of the correct π symmetry to back-bond to the CO ligand. It may be that it is the wedge shaped nature of the UCotCp fragment that accounts for the different results found for UCotCpCO. However, it would

Table 1 Structural parameters and spin densities (SD) for UCotCpCO with different functionals, basis sets and relativistic approximations

	U–C/Å	C–O/Å	SD U	SD C(CO)	SD O(CO)
BP86/TZP	2.381	1.173	2.73	0.27	0.14
BP86/SDD	2.395	1.175	2.80	0.19	0.13
B3LYP/TZP	2.485	1.149	2.85	0.19	0.10
B3PW91/SDD	2.214	1.049	2.73	0.18	0.15

Table 2 U–C, C–O, U–O and C–C distances (Å), spin densities and SCF energies relative to **2** (kJ mol^{-1}) calculated for intermediates and transition states in ynediolate formation

	U–C	C–O	U–O	C–C	U···U	SD U	SD C	SD O	Energy
2	2.381	1.173	n/a	n/a	n/a	2.72	0.27	0.14	0
5	2.322	1.221	2.491	2.614	4.42	2.00	0.11	0.05	–30
6*	2.310	1.264	2.350	1.917	4.72	1.93	0.16	0.05	–21
7	2.456	1.310	2.291	1.409	4.49	2.04	0.13	0.02	–48
8*	(3.904)	1.300	2.218	1.282	6.91	2.21	–0.02	–0.05	11
9	n/a	1.284	2.163	1.221	8.09	2.21	–0.03	–0.06	–4

be reassuring to have an experimental probe of the location of the spin density and epr may be useful in this context.

$[UCotCp]_2C_2O_2$

Reaction of UCotCp with a 1 : 1 stoichiometric quantity of CO leads to isolation of the yne diolate $[UCotCp]_2C_2O_2$. The initial C–C bond forming process is of particular interest. Many avenues for formation of the yne diolate were explored. Structures were optimized for $[Ucotcp]_2CO$, $Ucotcp(CO)_2$ and $[UcotcpCO]_2$ with a wide range of starting geometries. Comparison of the energetics yielded the low energy pathway described below. UCotCpCO can dimerize through coordination of the CO O atoms to the opposing U atoms. The intermediate formed, **5**, has C_i symmetry and a minimum energy with four unpaired electrons. The SCF energy is 0.29 eV lower than two monomeric units.

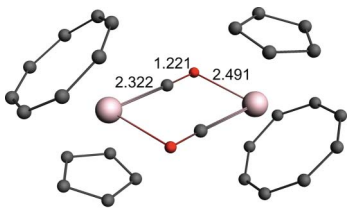

5

On dimerization the CO distance lengthens to 1.22 Å and the CO stretches drop to 1544 cm^{-1}. The C–C distance across the bridge is 2.61 Å. The isosurfaces for the six highest energy electrons are shown in Fig. 4. The two highest half occupied orbitals, 46a_g and 45a_u, are of 5f character and U localized. The next lowest in energy with unpaired spins, 45a_g and 44a_u, are of π symmetry with respect to the $U_2(CO)_2$ plane and represent in-phase and out-of-phase combinations of the U CO π* back-bonding orbitals. They are separated by 0.36 eV in energy. The next two electrons are paired in a σ symmetry orbital with respect to the $U_2(CO)_2$ plane, 44a_g, which is an in-phase combination of U CO π* back-bonding orbitals. The long distance between the two carbons does not at this stage indicate a bond despite the net in-phase interaction between them.

The path to C–C bond formation was explored by investigating the C–C distance as a potential reaction coordinate. Optimisations were carried out with a sequence of C–C distances and the maximum energy structure was subjected to a frequency calculation. The spin state of $S = 2$ was held throughout. The presence of one imaginary frequency with motion along the presumed reaction coordinate indicated that a transition state had been found. A transition state was identified, **6***, which led to a C_2O_2 "zig-zag" complex, **7**.

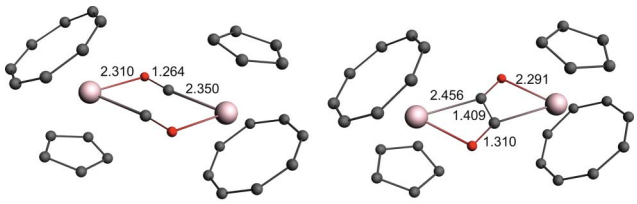

6* **7**

The C–C distance shortened to 1.92 Å in the transition state **6*** and to 1.41 Å in the zig-zag complex **7**. The corresponding distances are summarized in Table 2. As the C–C distance shortens the C–O distance lengthens.

In addition, the changes in the U–C and U–O bond lengths indicate that on moving from the dimer to the zig-zag complex the U–O bonding outweighs the U–C bonding.

The C–C distance in **7** is similar to that in benzene and indicates a bond order intermediate between a single and a double bond. The occupancy of the 44a_u and 44a_g changes along the series (Fig. 4). In the case of **5** 44a_u is singly occupied whereas 44a_g is doubly occupied whereas for **7** 44a_u is doubly occupied whereas 44a_g is singly occupied. For **7** orbital 45a_g is no longer C–C anti-bonding the electrons having retreated to the U 5f orbitals.

The U–C distances in the zig-zag complex, **7**, indicate that the U are still bonded to their respective carbons. This presumably presents an activation barrier to formation of the yne diolate, **9**. A search for a pathway from **7** to **9** revealed a possible transition state **8*** in which the C_2O_2 bridge has started to uncurl.

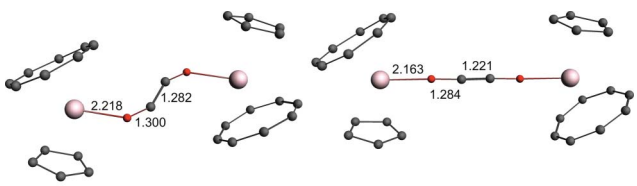

8* **9**

In **8*** the distance between a U and the C to which it was previously bonded has lengthened to such an extent that the bond has broken. The C–C distance has shortened considerably and is between that expected for a double and a triple bond (Table 2). The dimensions of the yne diolate bridge in **9** are comparable to those found in the crystal structure of $[U((\eta\text{-}C_8H_6\{Si^iPr_3\text{-}1,4\}_2)(\eta\text{-}C_5Me_5)]_2(C_2O_2)$[12] and the X-ray structure of the sodium salt $Na_2C_2O_2$.[22] In **9** the four unpaired electrons are localized in U5f orbitals (Fig. 4) and the spin density on the bridge is very low and of opposite sign to that of the unpaired electrons, demonstrating spin polarization rather than spin delocalization. The top doubly occupied orbital, 44a_u, corresponds to the HOMO of $C_2O_2^{2-}$ from which charge is donated to the U atoms.

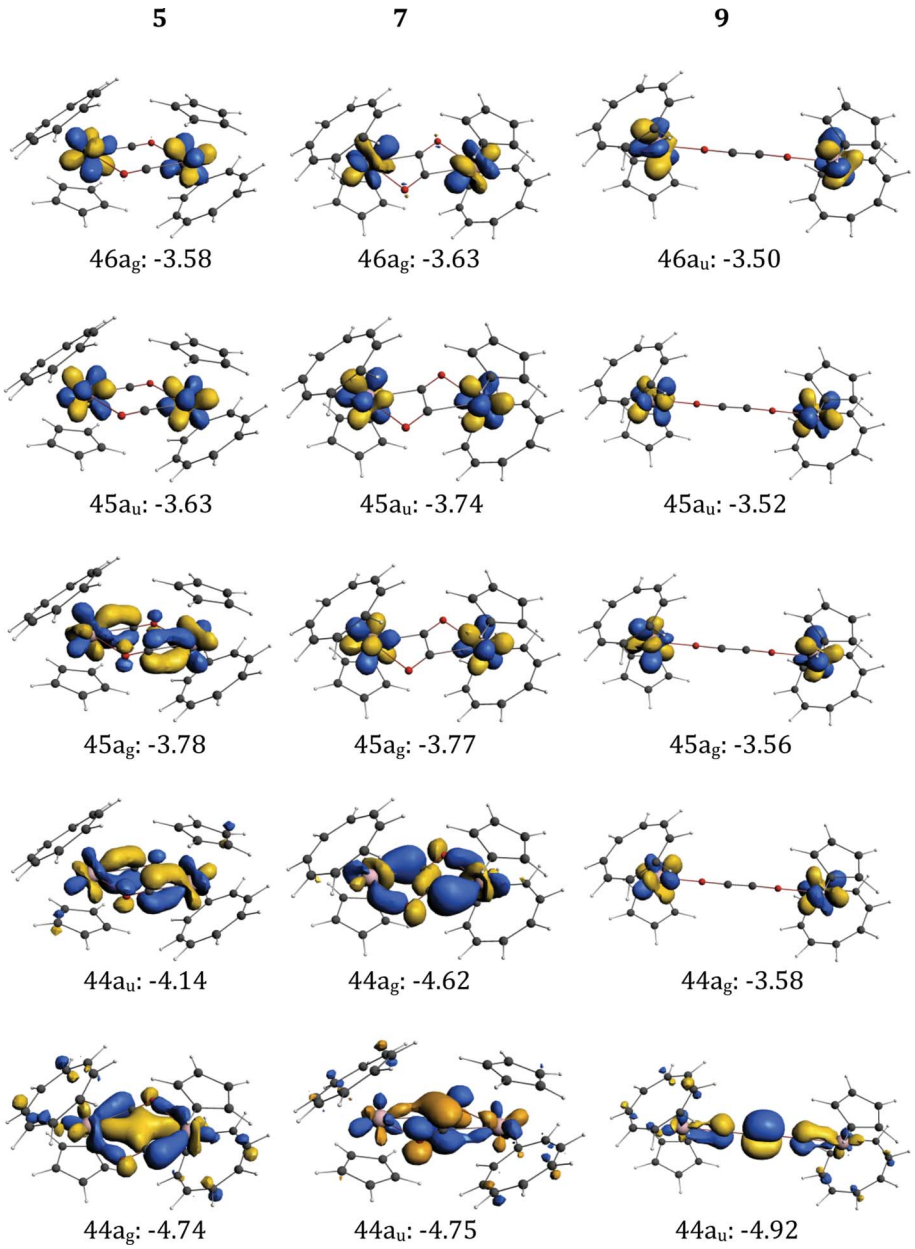

Fig. 4 Iso-surfaces and Kohm–Sham energies (eV) for upper alpha spin occupied orbitals of **5**, **7** and **9**. In each case the top four are singly occupied and account for the four unpaired spins. The lowest in energy is doubly occupied, the beta spin orbital having a comparable probability distribution.

Comparison of the energy pathway (Table 2) with the experimental results suggests the following reaction profile. UCotCp reacts with CO to form a monocarbonyl, UCotCpCO; this gives rise to the CO stretch observed on initial reaction. Two monocarbonyls join to form the dimer $[UCotCpCO]_2$. A low activation energy is then overcome to make the zig-zag complex. The activation energy barrier for formation of the yne diolate is somewhat higher ensuring that the zig-zag complex has a reasonable life time at low temperature. At room temperature the yne diolate is formed over a period of hours.

The energetics given in Table 2 are SCF energies which form the basis for characterizing the minima and transition states on the reaction pathway. The main discrepancy with experiment is the higher energy of **9** compared with **7** indicating our model, though suggestive, is deficient. The most likely cause of the departure is the absence of very bulky substituents in the model. The U···U distance in **5** and **7** (Table 2) is between 4 and 5 Å suggesting that in reality steric strain introduced by the tris-isopropylsilyl substituents would be significant. Such strain would be relieved in the yne diolate product with the longer U···U distance of >8 Å.

The necessary orbital transformations from two CO^- radical anions to the yne diolate dianion is best followed by examination of the bridging unit in isolation. Energies were calculated for the three minimum energy structures found for the bridge in **5**, **7** and **9** in C_{2h} symmetry. The orbital energies are shown in Fig. 5a and isosurfaces for selected orbitals in Fig. 5b.

The $5a_g$ and $2a_u$ orbitals are seen to be important components of $44a_g$ and $44a_u$ respectively (Fig. 4). However, in the case of the

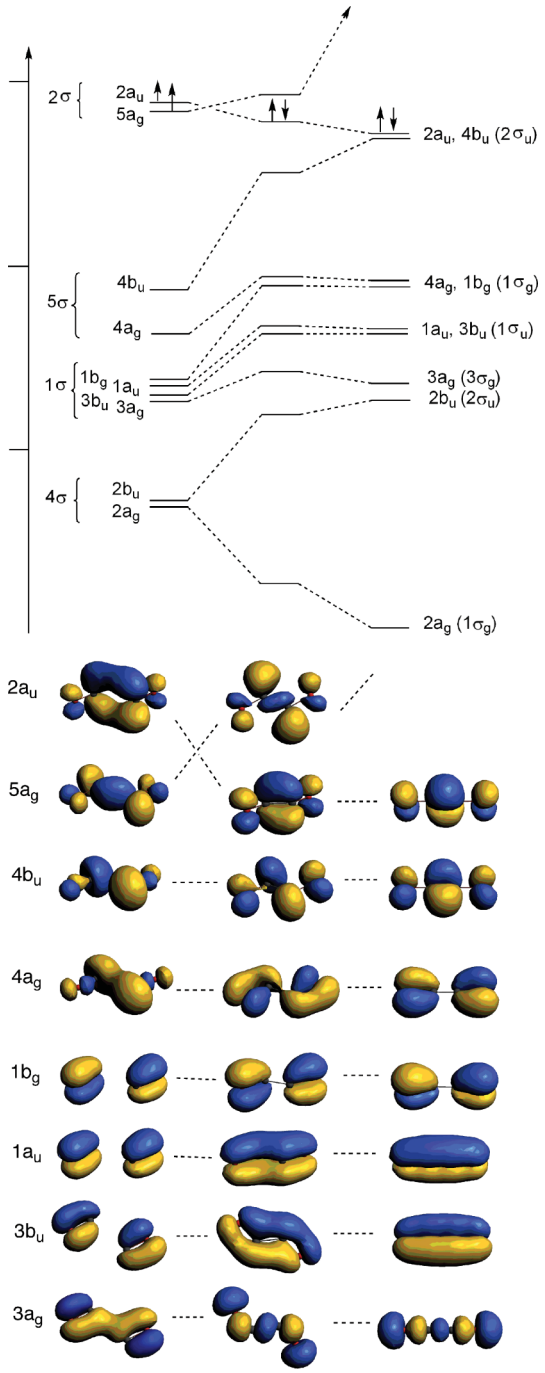

Fig. 5 (a) Calculated energy correlation of MOs of $[C_2O_2]^{2-}$ bridging unit in C_{2h} symmetry with geometry of dimer **5**, zig-zag, **7** and yne diolate, **9** structures. The dimer and linear structures are also labelled in linear symmetry (b) Iso-surfaces for upper orbitals.

U dimers charge is delocalized onto the U centres relieving the high energy of these orbitals. The two orbitals crossover in energy between the dimer and zig-zag configurations in both the isolated dianion and the diuranium complexes. The $2a_u$ orbital evolves smoothly into one of the upper π_u orbitals of the yne diolate. The other, $4b_u$, is formed from the anti-bonding combination of the in-plane combination of the CO 5σ orbitals, mixed with lower energy orbitals of b_u symmetry.

$[UCotCp]_2C_3O_3$

Experiment shows that the yne diolate complex is inert to further reaction with CO.[12] Thus the pathway to the deltate complex cannot proceed from the yne diolate. The presence of a stable intermediate, other than a monocarbonyl is also strongly implicated in the experimental results. The inference is that it is the stable intermediate which reacts with further CO to form the deltate complex and the computational study strongly suggests that the intermediate involved is the zig-zag complex, **7**.

The C_2O_2 dianion in the conformation imposed by the structure **7** has close lying HOMO and LUMO orbitals, $2a_u$ and $5a_g$ respectively. These are ideally set up for interaction with the HOMO and a LUMO of CO. The CO 5σ orbital can donate to $5a_g$ and a CO 2π orbital can accept electrons from $2a_u$. Adding CO to $[C_2O_2]^{2-}$ gave a Y-shaped structure, **10**. The deltate dianion, **11**, which is calculated to be 151 kJ mol^{-1} lower in energy, can be formed from **10** by making a third C–C bond. An activation energy of 75 kJ mol^{-1} was found for this process.

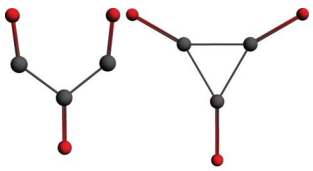

10 **11**

Problems with SCF convergence prevented tracing a pathway for the addition of CO to **7**. Instead the reaction was studied using thorium in place of uranium. Given that, on dimerisation, oxidation of the metal centres has largely taken place, the use of thorium should be indicative of a possible mechanism.

Addition of CO to one of the bridge carbons of $[ThCotCp]_2C_2O_2$, the Th analogue of **7** gave an intermediate with a Y shaped bridge asymmetrically bonded between the two Th atoms, **12**. The asymmetry arises because one of the bridge carbons is loosely bound to a Th atom. The other Th atom is attached to the bridge *via* two O atoms.

Formation of the deltate dianion from this intermediate passed through a transition state, **13***, 82 kJ mol^{-1} higher in energy than **12** and then formed a dimer with a similar structure to the U analogue **14** described below. For Th the process was exoenergetic by 51 kJ mol^{-1}.

Key distances calculated for the structure of the delate dianion in the U dimer uranium, **14**, are shown in Fig. 6 where they are compared with the experimental values for $[U(\eta\text{-}C_8H_6\{Si^iPr_3\text{-}1,4\}_2)(\eta\text{-}C_5Me_5)]_2(C_3O_3)$.

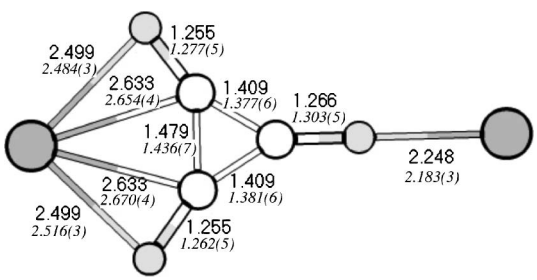

Fig. 6 Comparison of distances (Å) calculated for **14** and *crystal structure values* for $[U(\eta\text{-}C_8H_6\{Si^iPr_3\text{-}1,4\}_2)(\eta\text{-}C_5Me_5)]_2(C_3O_3)$.

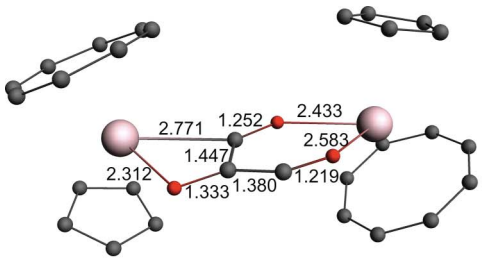

12

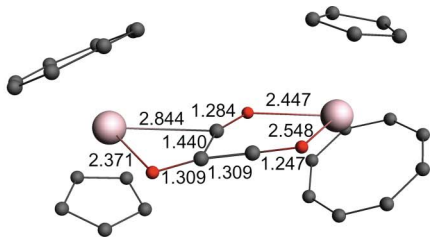

13

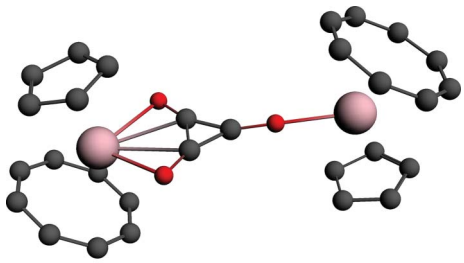

14

Of particular interest is the departure from three-fold symmetry shown by the deltate fragment, which shows one longer and two shorter C–C bond lengths and two shorter and one longer C–O bond length. This variation is well mirrored by the calculation. Examination of the orbital manifold of **14** shows that one of the degenerate e′ C–C bonding orbitals of $[C_3O_3]^{2-}$ interacts directly with a U atom forming an agostic C–C bond (51a′, Fig. 7). The other just donates through the O atoms (32a″, Fig. 7).

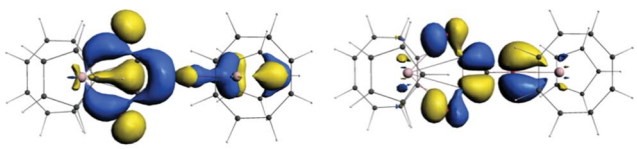

Fig. 7 Interaction of degenerate e′ C–C bonding orbitals of $[C_3O_3]^{2-}$ with UCotCp fragments: 51a′ shows a C–C agostic interaction with one of the U atoms.

The donation demonstrated in 51a′ will lengthen the associated C–C bond and shorten the C–O bonds as is found experimentally.

$[UCotCp]_2C_4O_4$

The squarate dimer is formed when the supporting cyclopentadienyl ligand is C_5Me_4H. Reaction of $U((\eta\text{-}C_8H_6\{Si^iPr_3\text{-}1,4\}_2)(\eta\text{-}C_5R_5)$ with CO is much faster than with C_5Me_5 as the supporting ligand. It is presumed that the smaller steric protection enables two CO molecules to react more rapidly with the zig-zag intermediate.

Such a reaction has been modelled in isolation. A minimum energy structure, **15**, was found with the two added CO groups *trans* to one another as would be anticipated with the zig-zag bridge. Rotation about the central C–C bond, moving through a transition state 6 kJ mol^{-1} higher in energy, positions the added CO groups in a *cis* orientation and C–C coupling ensues to form the squarate dianion, **16**, 322 kJ mol^{-1} more stable than **15**.

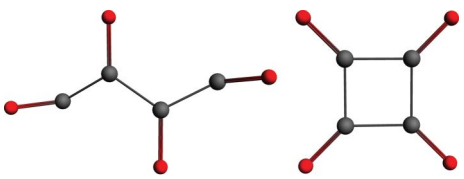

15 16

A possible intermediate, **17**, in formation of the squarate complex, was modelled for $[ThCotCp]_2C_4O_4$.

Two pathways were found for formation of a squarate complex from **17**. In one the Th–O bonds were retained and the central C–C bond was disrupted, C1 becoming bound to C3 and C2 to C4 (Scheme 3). An activation energy of 75 kJ mol^{-1} was found for this route. In the alternative pathway the two longer Th–O bonds were stretched and these O atoms decoordinated and C1 became bonded to C4 *via* rotation around the central C2–C3 bond (Scheme 3). The associated transition state, **18***, led to a complex with the squarate dianion coordinated through only two oxygens; further rearrangement, of lower energy, gave a $(\mu\text{-}\eta^2\text{:}\eta^{22}\text{-}C_4O_4)$ product. The activation energy for this process was lower at 13 kJ mol^{-1}.

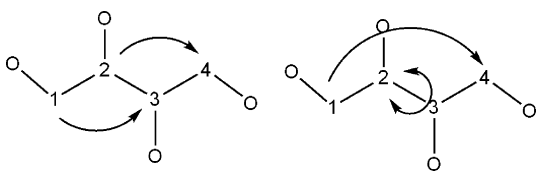

Scheme 3

The low energy for decoordination of the O atoms may be explained by their carbonyl nature and the long initial distance.

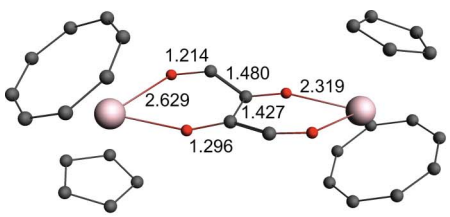

17

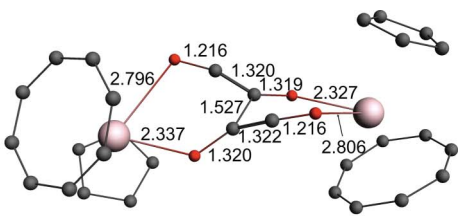

18*

Thus this pathway appears to be preferable. Overall formation of the Th squarate dimer from **17** was exoenergetic by 275 kJ mol^{-1}.

The structure of $[UCotCp]_2C_4O_4$ was optimized with a centre of inversion, **19**.

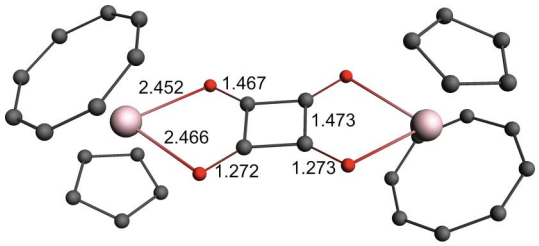

19

In the case of **19** the interaction between the bridging dianion and the U atoms was exclusively through the coordinating O atoms and there was no interaction with the C–C bonds of the four membered ring. The bond distances were comparable to those found experimentally.[11]

Conclusions

The ability for UCotCp to form the zig-zag dimer is crucial for facilitating the CO reductive coupling reactions found experimentally. Prerequisites for this dimer formation are delocalization of unpaired spin density onto CO in the initial monocarbonyl formation and the subsequent coordination of a pair of CO O atoms to the opposing U atoms in initial dimer formation. The subsequent fate of the dimer depends on the further availability of CO and the steric constraints of the supporting ligands. Lack of additional CO results in yne diolate formation. When C_5Me_5 is the supporting ligand, reaction with one further molecule of CO gives a Y-shaped bridging intermediate, which readily forms the deltate dianion dimer. Surprisingly, one of the C–C bonds in the bridging delate is lengthened due to a C–C agostic interaction with a U atom. The less constricted steric environment of C_5Me_4H allows two further molecules of CO to react with the zig-zag complex resulting in the squarate dimer. The low temperature stabilization of the zig-zag complex suggests the possibility of reaction at the C atoms with other small molecules. Such an intermediate is a possible candidate for the formation of a methoxide complex when $U((\eta\text{-}C_8H_6\{Si^iPr_3\text{-}1,4\}_2)(\eta\text{-}C_5Me_5)$ is reacted with a mixture of CO and H_2.[23]

Computational methods

Unless otherwise stated density functional calculations were carried out using the Amsterdam Density Functional program suites ADF 2004.04 and ADF 2010.2.[24–26] Scalar relativistic corrections were included *via* the ZORA method for all calculations.[27–30] The generalized gradient approximation was employed, using the local density approximation of Vosko, Wilk, and Nusair[31] together with non-local exchange correction by Becke[32,33] and non-local correlation corrections by Perdew.[34] TZP basis sets were used with triple-ζ accuracy sets of Slater type orbitals and polarization functions added to the main group atoms. The cores of the atoms were frozen up to 1s for C and O, and 5d for U. Default conditions were used for the optimizations and frequency calculations. Some of the optimized structures had small imaginary frequencies associated with the barrierless rotation of the C_8H_8 rings. Otherwise proposed transition states showed one imaginary frequency with motion along the proposed reaction coordinate. The optimized Cartesian coordinates for the reported structures are given in the ESI.† Calculations including spin–orbit coupling were carried out previously for **2** and **5–9**[12] the results, which were reported in the ESI,† gave a similar but more generally exoenergetic energy profile.

Calculations were also performed on UCotCpCO using the ADF suite and the B3LYP[31,35–37] functional and the Gaussian program suite.[21] The latter employed both the BP86,[31–34] and B3PW91[38–43] functional; a (14s13p10d 8f)/[10s9p5d4f] segmented valence basis set with Stuttgart–Bonn variety relativistic effective core potential was used for U[44] and Dunning's ccpVDZ basis sets were employed for the non f elements.

Spin densities and orbital decomposition were engendered by a Mulliken population analysis. Iso-surfaces are drawn at a level of 0.04.

Acknowledgements

We thank EPSRC for financial support and the Oxford Supercomputing Centre for facilities.

References

1 F. Fischer and H. Tropsch, *Chem. Ber.*, 1926, **59**, 830.
2 *Advances in Fischer–Tropsch Synthesis, Catalysts and Catalysis.*, ed. B. H. Davis and M. L. Occelli, CRC Press, Washington DC, 2009.
3 B. Wayland and X. Fu, *Science*, 2006, **311**, 790 and references therein.
4 D. R. McAlister, R. D. Sanner and J. E. Bercaw, *J. Am. Chem. Soc.*, 1976, **98**, 6733.
5 P. J. Fagan, K. G. Moloy and T. J. Marks, *J. Am. Chem. Soc.*, 1981, **103**, 6959.
6 W. J. Evans, J. W. Grate and R. J. Doedens, *J. Am. Chem. Soc.*, 1985, **107**, 1671.
7 T. Shima and Z. Hou, *J. Am. Chem. Soc.*, 2006, **128**, 8124.
8 W. J. Evans, J. W. Grate, L. A. Hughes, H. Zhang and J. L. Atwood, *J. Am. Chem. Soc.*, 1985, **107**, 3728.
9 W. J. Evans, D. S. Lee, J. W. Ziller and N. Kaltsoyannis, *J. Am. Chem. Soc.*, 2006, **128**, 14176.
10 O. T. Summerscales, F. G. N. Cloke, P. B. Hitchcock, J. C. Green and N. Hazari, *Science*, 2006, **311**, 829–831.
11 O. T. Summerscales, F. G. N. Cloke, P. B. Hitchcock, J. C. Green and N. Hazari, *J. Am. Chem. Soc.*, 2006, **128**, 9602–9603.
12 A. S. Frey, F. G. N. Cloke, P. B. Hitchcock, I. J. Day, J. C. Green and G. Aitken, *J. Am. Chem. Soc.*, 2008, **130**, 13816–13817.
13 M. Dolg and X. Cao, in *Encyclopedia of Inorganic Chemistry*, John Wiley & Sons, Ltd, Edition 2, 2006.
14 L. Gagliardi and B. O. Roos, *Chem. Soc. Rev.*, 2007, **36**, 893–903.
15 P. J. Hay and R. L. Martin, *Los Alamos Sci.*, 2000, **26**, 382–391.
16 N. Kaltsoyannis, *Chem. Soc. Rev.*, 2003, **32**, 9–16.
17 A. R. Schake, L. R. Avens, C. J. Burns, D. L. Clark, A. P. Sattelberger and W. H. Smith, *Organometallics*, 1993, **12**, 1497–1498.
18 J. Parry, E. Carmona, S. Coles and M. Hursthouse, *J. Am. Chem. Soc.*, 1995, **117**, 2649–2650.
19 W. J. Evans, S. A. Kozimor, G. W. Nyce and J. W. Ziller, *J. Am. Chem. Soc.*, 2003, **125**, 13831–13835.
20 L. Maron, O. Eisenstein and R. A. Andersen, *Organometallics*, 2009, **28**, 3629–3635.
21 M. J. Frisch, G. W. Trucks, H. B. Schlegel, G. E. Scuseria, M. A. Robb, J. R. Cheeseman, J. A. Montgomery, Jr., T. Vreven, K. N. Kudin, J. C. Burant, J. M. Millam, S. S. Iyengar, J. Tomasi, V. Barone, B. Mennucci, M. Cossi, G. Scalmani, N. Rega, G. A. Petersson, H. Nakatsuji, M. Hada, M. Ehara, K. Toyota, R. Fukuda, J. Hasegawa, M. Ishida, T. Nakajima, Y. Honda, O. Kitao, H. Nakai, M. Klene, X. Li, J. E. Knox, H. P. Hratchian, J. B. Cross, V. Bakken, C. Adamo, J. Jaramillo,

R. Gomperts, R. E. Stratmann, O. Yazyev, A. J. Austin, R. Cammi, C. Pomelli, J. Ochterski, P. Y. Ayala, K. Morokuma, G. A. Voth, P. Salvador, J. J. Dannenberg, V. G. Zakrzewski, S. Dapprich, A. D. Daniels, M. C. Strain, O. Farkas, D. K. Malick, A. D. Rabuck, K. Raghavachari, J. B. Foresman, J. V. Ortiz, Q. Cui, A. G. Baboul, S. Clifford, J. Cioslowski, B. B. Stefanov, G. Liu, A. Liashenko, P. Piskorz, I. Komaromi, R. L. Martin, D. J. Fox, T. Keith, M. A. Al-Laham, C. Y. Peng, A. Nanayakkara, M. Challacombe, P. M. W. Gill, B. G. Johnson, W. Chen, M. W. Wong, C. Gonzalez and J. A. Pople, *GAUSSIAN 03 (Revision D.02)*, Gaussian, Inc., Wallingford, CT, 2004.

22 E. Weiss and W. Buchner, *Chem. Ber.*, 1965, **98**, 126.

23 F. G. N. Cloke, A. S. Frey, M. P. Coles, L. Maron and T. Davin, *Angew. Chem., Int. Ed.*, 2011, **50**, 6881–6883.

24 ADF2004.01 ADF2010.02, Theoretical Chemistry, Vrije Universiteit, Amsterdam, The Netherlands, http://www.scm.com.

25 G. te Velde, F. M. Bickelhaupt, E. J. Baerends, C. Fonseca Guerra, S. J. A. Van Gisbergen, J. G. Snijders and T. Ziegler, *J. Comput. Chem.*, 2001, **22**, 931.

26 C. Fonseca Guerra, J. G. Snijders, G. te Velde and E. J. Baerends, *Theor. Chem. Acc.*, 1998, **99**, 391.

27 E. van Lenthe, E. J. Baerends and J. G. Snijders, *J. Chem. Phys.*, 1993, **99**, 4597.

28 E. van Lenthe, E. J. Baerends and J. G. Snijders, *J. Chem. Phys.*, 1994, **101**, 9783.

29 E. van Lenthe, J. G. Snijders and E. J. Baerends, *J. Chem. Phys.*, 1996, **105**, 6505.

30 E. van Lenthe, R. van Leeuwen, E. J. Baerends and J. G. Snijders, *Int. J. Quantum Chem.*, 1996, **57**, 281.

31 S. H. Vosko, L. Wilk and M. Nusair, *Can. J. Phys.*, 1980, **58**, 1200.

32 A. D. Becke, *Phys. Rev. A: At., Mol., Opt. Phys.*, 1988, **38**, 3098.

33 A. D. Becke, *J. Chem. Phys.*, 1988, **88**, 1053.

34 J. P. Perdew, *Phys. Rev. B*, 1986, **33**, 8800.

35 A. D. Becke, *J. Chem. Phys.*, 1993, **98**, 5648–5652.

36 P. J. Stephens, F. J. Devlin, C. F. Chabalowski and M. J. Frisch, *J. Phys. Chem.*, 1994, **98**, 11623–11627.

37 C. Lee, W. Yang and R. G. Parr, *Phys. Rev. B*, 1988, **37**, 785–789.

38 J. P. Perdew, in *Electronic structure of solids*, ed. P. Ziesche and H. Eschrig, Akademie, Berlin, Editon edn, 1991.

39 J. P. Perdew, K. Burke and Y. Wang, *Phys. Rev. B: Condens. Matter*, 1996, **54**, 16533–16539.

40 K. Burke, J. P. Perdew and Y. Wang, in *Electronic density functional theory: recent progress and new directions*, ed. J. F. Dobson, G. Vignale and M. P. Das, Plenum, New York, Editon edn, 1998.

41 J. P. Perdew, J. A. Chevary, S. H. Vosko, K. A. Jackson, M. R. Pederson, D. J. Singh and C. Fiolhais, *Phys. Rev. B: Condens. Matter*, 1992, **46**, 6671–6687.

42 J. P. Perdew, K. Burke and Y. Wang, *Phys. Rev. B: Condens. Matter*, 1998, **57**, 14999.

43 J. P. Perdew, J. A. Chevary, S. H. Vosko, K. A. Jackson, M. R. Pederson, D. J. Singh and C. Fiolhais, *Phys. Rev. B: Condens. Matter*, 1993, **48**, 4978.

44 X. Y. Cao and M. Dolg, *THEOCHEM*, 2004, **673**, 203.

